Title

Applications of Combined X-Ray Photoelectron/Auger Spectroscopy to Studies of Inorganic Materials

Author

Perry, Dale L.

Publication Date

1992-03-01

LBL-32058
UC-108

Lawrence Berkeley Laboratory
UNIVERSITY OF CALIFORNIA

EARTH SCIENCES DIVISION

To be published as a chapter in *Applications of Analytical Techniques to the Characterization of Materials*, Dale L. Perry, Ed., Plenum Publishing Corp., New York, NY, 1992

Applications of Combined X-Ray Photoelectron/Auger Spectroscopy to Studies of Inorganic Materials

D.L. Perry

March 1992

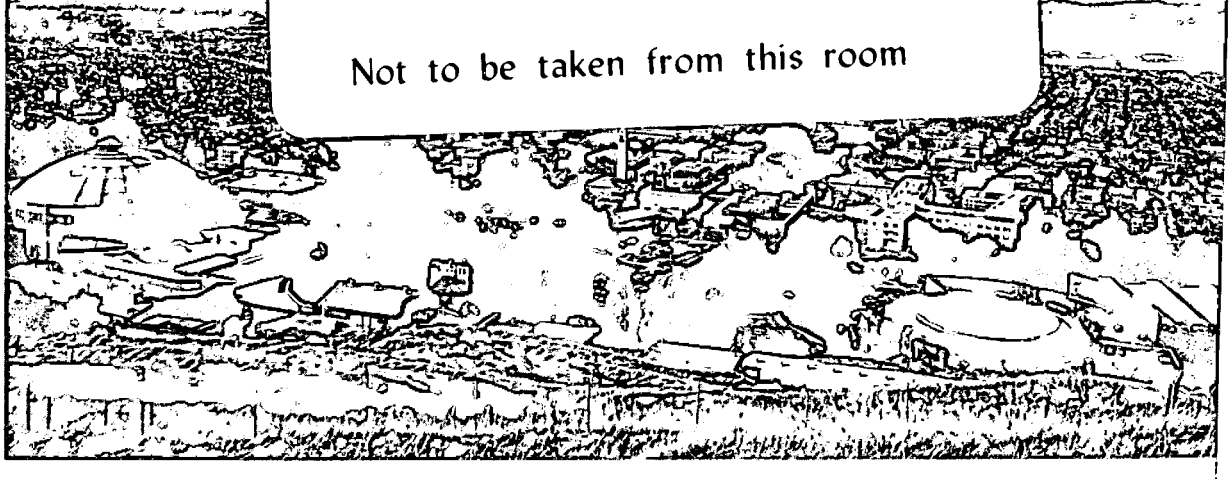

Prepared for the U.S. Department of Energy under Contract Number DE-AC03-76SF00098

DISCLAIMER

LBL-32058

Applications of Combined X-Ray Photoelectron/Auger Spectroscopy to Studies of Inorganic Materials

Dale L. Perry

Earth Sciences Division
Lawrence Berkeley Laboratory
University of California
Berkeley, California 94720

March 1992

Published in *Applications of Analytical Techniques to the Characterization of Materials*. Edited by Dale L. Perry, Plenum Publishing Corporation, New York, 1992.

This work was supported by the Assistant Secretary for Fossil Energy, Office of Oil, Gas and Shale Technologies, under U.S. Department of Energy Contract No. DE-AC03-76SF00098, through the Morgantown Energy Technology Center, Morgantown, West Virginia, and the Center for Science and Engineering Education, Lawrence Berkeley Laboratory, University of California.

APPLICATION OF COMBINED X-RAY PHOTOELECTRON/ AUGER SPECTROSCOPY TO STUDIES OF INORGANIC MATERIALS

Dale L. Perry

Lawrence Berkeley Laboratory
University of California
Berkeley, CA 94720

1. INTRODUCTION

Many materials that are of interest to materials scientists are inorganic in nature. Some of the more common ones are nitrides (Ni_3N_3), arsenides (GaAs), intermetallic compounds (Ni_3Al), metallic carbides (CaC_2), and multimetal mixed oxides (relatively recent superconductors such as $YBa_2Cu_3O_7$ and their related compounds). As is the case with all materials, a researcher is very interested in studying many facets of the characterization of the solids, including lattice structure, bonding, and electronic structure. In order to obtain types of information such as these, a variety of experimental approaches must be used. No single type of instrumentation can give a total picture of a material, but several techniques can complement one another to contribute pieces of the description.

One of the most potent techniques for the characterization of inorganic materials is that of combined x-ray photoelectron/Auger spectroscopy, this combination offering several advantages. First, an investigator has two techniques at his disposal while only using one type of instrumentation: the x-ray source that generates the x-ray photoelectron spectrum for a given energy range also generates complementary Auger spectra for other elements in the material for those Auger lines that are attainable in the same energy range.

Second, several diverse types of materials can be studied. There are, for example, no exclusionary rules inherent to the physics of the experiment that allow one to look only at a diamagnetic *vs.* a paramagnetic solid. Indeed, as will be seen in the following discussion, the experimental approach allows for easy differentiation of such species in many cases. Also, a wide variety of *physical* types of materials is amenable to study by this approach. Hard refractory materials, polymers, and thin films—all can be studied readily.

Third, with the help of high quality elemental standards, the techniques are highly effective at providing both qualitative and quantitative information concerning atomic stoichiometries in materials. Care must be taken, of course, to use rigorously obtained sensitivities for the elements in very pure standard materials and that those sensitivities obtained are truly reflective of elemental concentrations in the material of interest.

Finally, combined x-ray photoelectron/Auger spectroscopy is extremely useful in the study of bonding exhibited by inorganic materials, bonding from both a structural and electronic standpoint. Most elements can be studied in a variety of bonding environments. Sulfur, for example, can be studied as a sulfate anion, with the sulfur in the +6 oxidation state, which has a definite electronic state and a well-understood structure in the solid state. Conversely, sulfur also exists as a sulfide, with the formal oxidation state of -2; this form also appears in solid materials in conjunction with other elements in known structural arrangements. Other elements exist in decidedly different structural and electronic states (e.g. UO_2^{2+} *vs.* U_2O_5, MoO_4^{2-} *vs.* MoO_2, Cu^+ *vs.* $CuCl_4^{2-}$) and can be studied by both x-ray photoelectron and Auger spectroscopy.

X-ray photoelectron and Auger spectroscopy are quite surface sensitive to elements (approximately 0.1-0.5% atomic concentration) in materials, but, using high quality samples which are surface clean and represent the bulk, the techniques are very effective at looking at materials which are vacuum-amenable (10^{-8} - 10^{-11} torr). Problems are encountered during the study of some samples, however, and these include surface sample charging,[1-3] metal ion reduction,[4-7] and dehydration of hydrated inorganic salts.[8] Careful monitoring of the spectra as a function of time and visual observation of the material surface can be used to assess these effects and experimentally adjust for them.

2. PRINCIPLES OF THE EXPERIMENT

The bases of the x-ray photoelectron and Auger spectroscopies are depicted in Figure 1, with the case of nitrogen (Z=7) being illustrated. Under vacuum, a solid surface is impinged on by soft x-rays (typically, either Mg $K\alpha$ x-rays at 1253.6 eV or Al $K\alpha$ x-rays at 1486.6 eV are used, but higher energy x-ray sources have also been employed to excite higher energy level core electron lines; some of these anodes include the Ti $K\alpha$ line (4510.9 eV), the Cr $K\alpha$ line (5414.7 eV), and the Ag $L\alpha$ line (2984.3 eV)), and the emitted photoelectrons are analyzed as a function of their kinetic energies. The photoelectrons will have kinetic energies, E_k, that are defined by the relationship in Equation 1

$$E_k = h\upsilon - E_b - \phi_s \qquad (1)$$

where E_b is the binding energy for a given level (in Figure 1, the binding energy for the shown ejected electron would be that of the nitrogen 1*s* level), ϕ_s is the spectrometer work function, and $h\upsilon$ is the energy of the impinging radiation.

An additional process also occurs as an after-effect of the electron photoemission, that process being the Auger process. The Auger effect is due to a relaxation process resulting in the emission of Auger electrons. Again, in Figure 1, for the case of the

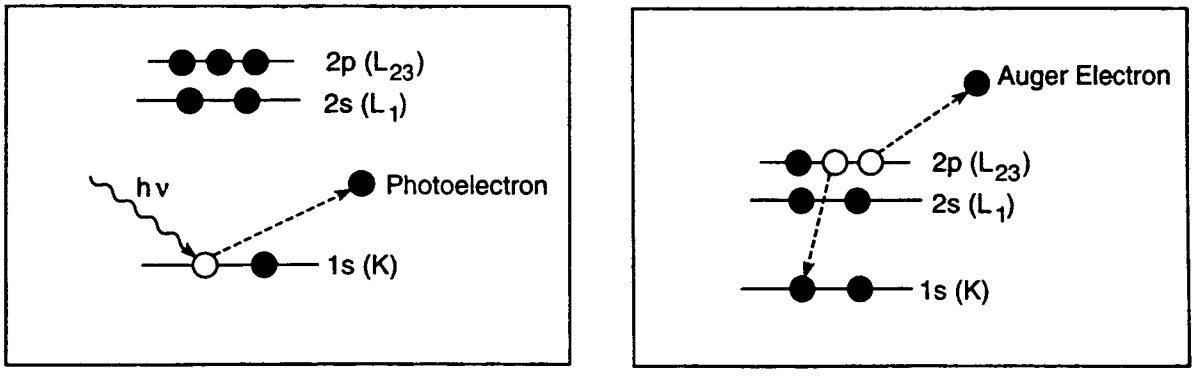

Figure 1. Electronic transitions involved in the x-ray photoelectron and Auger processes for the nitrogen atom. (XBL 8812-105600)

nitrogen atom, the empty hole in the 1*s* (also sometimes designated as the *K* shell) level is filled by an electron from the 2*p* (*L*) shell; a second electron, the Auger electron, is then emitted from the same shell. Thus, for the Auger process, the three letters describe the process in terms of the shell from which the photoelectron evolves, the shell from which an electron fills the hole, and, finally, the shell from which evolves the Auger electron, respectively. Collectively, then, the observed Auger spectrum is referred to as the *KLL* spectrum. When the last two shells involve a valence shell as is the case here for nitrogen, the Auger transition is sometimes designated as the *KVV* transition. Thus, an investigator can observe two types of spectroscopy in the same experiment and use their various spectral features to study a solid material (Table 1).

The features of the combined x-ray generated photoelectron and Auger spectra can be seen in Figure 2 for the case of boron nitride, BN, a common inorganic material. First, the nitrogen 1*s* photoelectron line at 397.9 eV is observed. Second, the most intense Auger line in this energy range is that of the nitrogen *KVV* transition at 873.4 eV (on performing a high resolution study of this region of the spectrum, one also sees two other peak maxima at 890.6 and 903.0 eV, two peaks not well resolved in this ~1300 eV "survey" scan). For the study of nitrogen compounds, these are the sets of lines of interest. Other nitrogen compounds exhibit different values for these lines, the range of values being rather large for the types of compounds studied.

The purpose of the present work is twofold. First, combined x-ray photoelectron and Auger spectroscopic parameters exhibited by different materials will be discussed with respect to their significance in the study of bonding and structure of those materials. Second, actual studies of a variety of materials will be described, with each study demonstrating how the combined techniques can be used to obtain important information about materials. This treatise is meant as an overview of the application of these two spectroscopies to a wide variety of materials. As a result, there is no in-depth discussion

Table 1. Some Suitable X-Ray Photoelectron and Auger Lines for Studying Representative Inorganic Materials

Element	Photoelectron Line	Auger Line	Material Studied
Oxygen	1*s*	*KVV*	Oxides, oxyanions, and oxygen-donor ligand complexes.
Nitrogen	1*s*	*KVV*	Nitrides, azides, nitrogen-containing oxyanions, and N-donor ligand complexes
Arsenic	3*d*	*LMM*	Arsenic oxides, salts, arsenides, and As-containing oxyanions.
Silicon	2*p*	$K_{23}L_{27}$	Silicon salts, aluminosilicates, silicides, and silicates.
Aluminum	2*p*	$KL_{23}L_{23}$	Aluminum salts, aluminates, and aluminosilicates.
Tellurium	3*d*	$M_4N_{45}N_{45}$	Tellurium oxides, salts, tellurates, and tellurides.
Zinc	2*p*	$L_3M_{45}M_{45}$	Zinc oxides, salts, and coordination complexes.
Carbon	1*s*	*KVV*	Carbides, carbonates, and polymers.

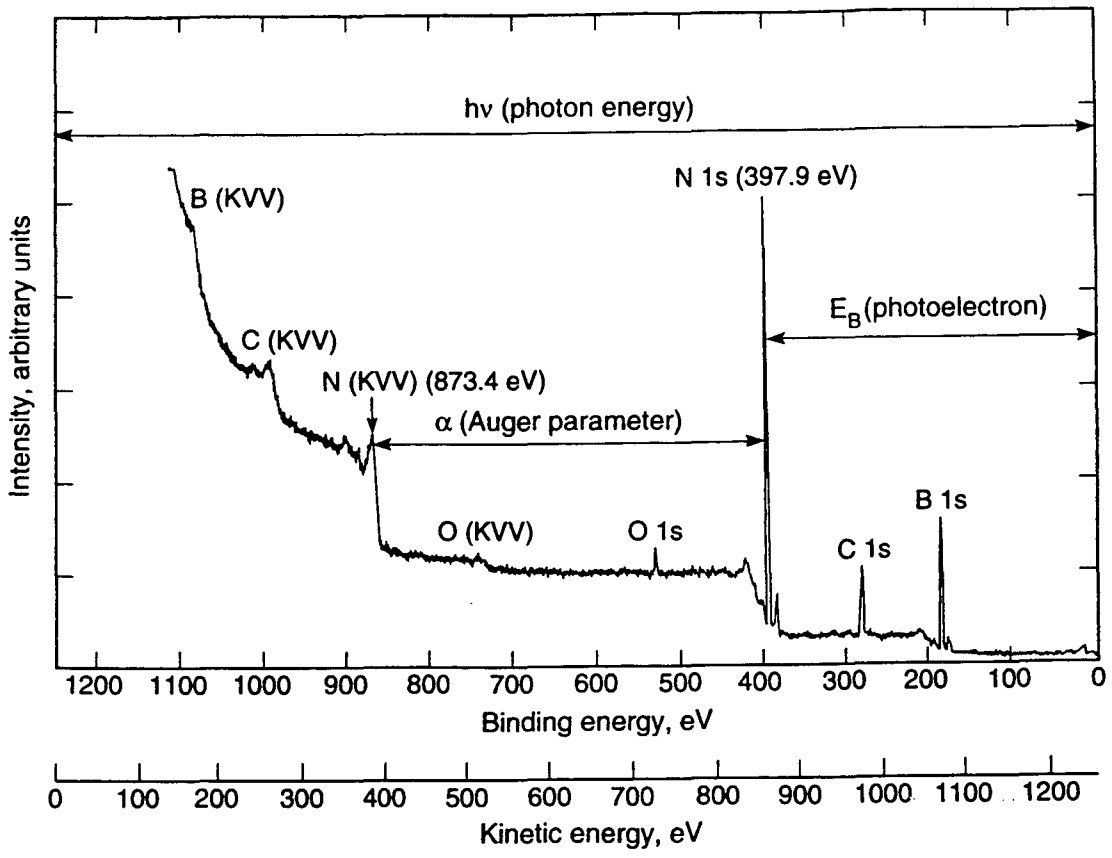

Figure 2. Survey scan of the combined x-ray photoelectron and Auger spectra of boron nitride, BN, using Mg *Ka* radiation. (XBL 896-7535A)

of individual classes of inorganic materials, i.e., ceramics, catalysts, glasses, etc. The reader is referred to the literature for more extensive discussions of these types of materials, since only various members will be used here for illustrative purposes; also, the reader should likewise consult more in depth treatises on x-ray induced photoelectron and Auger spectroscopy for a more comprehensive discussion of the basic principles than is possible in this relatively short work.[9-11]

3. SPECTROSCOPIC CHARACTERISTICS OF THE COMBINED X-RAY PHOTOELECTRON/AUGER SPECTRUM

3.1. Binding Energy

The numerical value of each of the x-ray photoelectron lines in Figure 2 is referred to as the binding energy of that line, and the general position of each of the sets of lines is specific for a particular element. Lines for some elements exhibit far greater shifts than do lines of other elements with respect to changes in chemical state for the elements. The range of binding energy shifts for photoelectron peaks can sometimes be quite large. In the case of sulfur mentioned above, the shift of the sulfur 2*p* line over all the possible chemical states encompasses ~6 eV. Other elements which have comparable binding energy ranges include oxygen, nitrogen, and silicon. Again using the nitrogen 1*s* for BN in Figure 2 as an example, the value of 397.9 eV represents the approximate low end of the binding energy scale for nitrogen. For the highest oxidation state of nitrogen (+5) in the NO_3^- functional group, the binding energy rises to ~406 eV for nitrates such as NH_4NO_3 and $NaNO_3$. In the case of NH_4NO_3 there are, of course, two types of nitrogen atoms, with the NH_4^+ nitrogen being observed at a binding energy of ~401 eV.

Other elements do not exhibit as wide a range of binding energies for their chemistries. Magnesium, for example, has a binding energy span for the metal and its binary compounds comprised of oxygen and fluorine of only about 3 eV for the $2p$ photoelectron line. Zinc also yields binding energies in a 2-3 eV range for its compounds.

The Auger shift of an element for its various compounds, however, can be much greater than the binding energy shifts for the same compounds. Some of the Auger line shifts can be two to ten times the shifts for some of the binding energies.[12] Cadmium, zinc, silver, copper, and magnesium display quite large Auger line shifts while exhibiting rather small x-ray photoelectron shifts. By studying the sets of x-ray photoelectron and Auger lines of an element, therefore, one can many times differentiate among several types of chemical species for that element. This will be discussed further below.

3.2. Spin-Orbit Splitting

Another spectroscopic parameter observed in combined x-ray photoelectron/Auger spectra is that of spin-orbit splitting. Upon ionization of an p, d, or f electronic shell in an atom, the photoelectron line splits into a doublet. The p level thus appears as the $p_{3/2,\,1/2}$ doublet, and d and f levels as the $d_{5/2,3/2}$ and $f_{7/2,5/2}$, respectively. This splitting can be observed in Figure 3 for the case of nickel(II) halides and some of their complexes. The

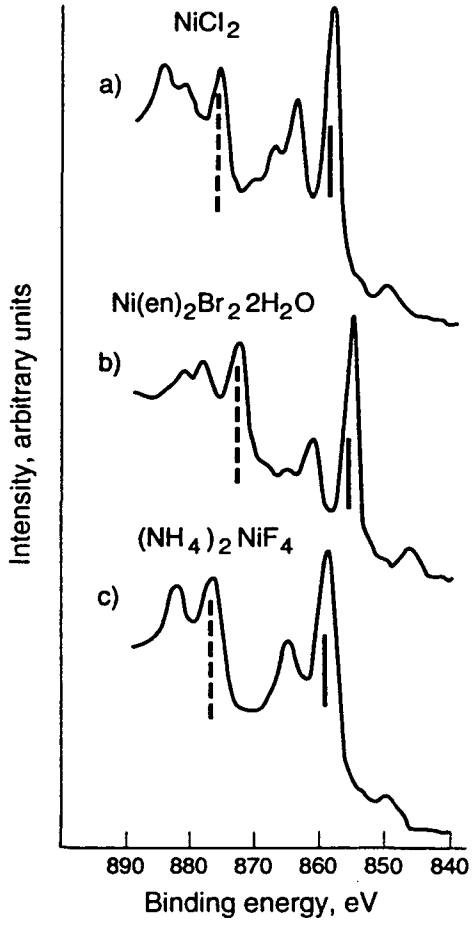

Figure 3. The nickel $2p_{3/2,1/2}$ photoelectron lines for several nickel(II) halides and their organic complexes. The solid, vertical line represents the $2p_{3/2}$ photoelectron line, while the broken, vertical line represents the $2p_{1/2}$ photoelectron line. Adapted from Reference 19. (XBL 914-6074)

more intense line in each doublet at the lower binding energy for each compound is the $2p_{3/2}$ photoelectron line, while the less intense line in each doublet is the $2p_{1/2}$ photoelectron line. In the *p*, *d*, and *f* spectra of most elements, the separation between the two states is constant; the separation is not observed as a function of such chemical state variables as oxidation state and chemical species (i.e., a sulfate *vs.* a sulfide). Some doublet lines are sometimes difficult to resolve in a spectrum. The sulfur $2p_{3/2,1/2}$ lines are only split by 1.2 eV and are often observed as a broadened peak, for example.

There are several chemical systems, however, in which the spin-orbit splitting *is* a function of different chemical species. The splitting difference varies by about one electron volt for high-spin cobalt(II) compounds and low-spin cobalt(III) compounds.[13] Other elements for which this splitting changes are uranium[14] and lead.[15]

3.3. Satellite Structure

Another spectroscopic phenomenon exhibited by some inorganic materials is that of satellite structure. Satellite structure for an element results from coupled electronic processes during the ionization process of that element in a material. During the ionization depicted in Figure 1 for an element, a "hole" is created in the orbital level. If the kinetic energy of the primary ejected electron creating this hole is shared with valence electrons to promote another electron to an excited state, the process manifests itself as satellite structures to the high binding energy side of the main photoelectron lines and is called a "shake-up" satellite. If, however, this sharing of energy with valence electrons results in the promotion of another electron to a continuum state, the satellite results from a "shake-off" process. Both processes are types of electronic configuration interactions. While these processes can be described using a quantum mechanical approach, the discussion here will be restricted to using the spectral phenomena for differentiating among different chemical species in inorganic solids. A more rigorous discussion can be found in the literature.[16-18]

Satellite structure can be observed for elemental species in which the central element is in either a diamagnetic or paramagnetic compound, the satellite being almost nonexistent or not observed at all. For elements that are paramagnetic, however, the satellite structure can be quite intense. In Figure 3, quite strong features can be seen to the high binding energy sides of the main nickel(II) $2p_{3/2,1/2}$ lines.[19] Note, however, that the satellites are not identical to each other for the three compounds shown and are unique for each compound. This observation is extremely important for both the characterization of inorganic materials and sorting out different chemical species that might be formed in their processing and any reactions they subsequently undergo.

Even among the thousands of inorganic species that have been studied, certain trends can be observed for satellite structure. Vernon and co-workers[20] have reported quite an extensive study of transition metal oxides, halides, and some transition metal complexes.

Some of these observations for transition metal species are as follows.

1. Pure metals do not show strong satellite features.
2. The metal oxides exhibit metal 2*p* photoelectron spectra that have well-defined satellite peaks associated with them.
3. Minor satellite structure is associated with the spectra of transition metal complexes with the cyano (CN^-) ligand.
4. The transition metal halides show strong satellites at higher binding energy to the 2*p* lines.
5. The most intense satellites for the metal 2*p* photoelectron lines are observed for paramagnetic compounds and compounds of high-field ligands, excluding d^0 compounds of titanium and scandium.

6. The intensity of the $2p$ satellites increases for the $3d$ transition metals as the atomic number of the metal increases.
7. Second and third row transition metal compounds do not exhibit $2p$ satellite structure attributable to electron shake-up processes; this is possibly due to second-and third-row transition metal compounds as having high crystal field splitting and high spin-orbit coupling.

Another mechanism that is responsible for satellite structure in conjunction with shake-up processes is that of charge transfer. One example of this process being operable is that of the uranium system. In the case of UO_2, the uranium is in the tetrapositive state, with a formal electronic configuration of $5f$.[2] The molecule exhibits a $4f_{7/2,5/2}$ spectrum with two satellites, with one of them related to the shake-up excitation of an electron from the donor oxygen atom $2p$- uranium bonding band to the partially filled localized metal $5f$ level.[21-23] This same phenomenon is observed in uranium spectra involving the diamagnetic uranyl ion, UO_2^{2+}, which is formally a $5f^0$ species with no unpaired electrons. Figure 4 shows the spectrum of a uranyl complex[24] reported by Perry in which the donor set of ligand atoms consists of both oxygen and sulfur atoms. Again, satellite structure is quite pronounced, along with the nitrogen $1s$ photoelectron line.

Other diamagnetic species which exhibit satellite structure are the $5f^0$ system ThO_2[25] and CeO_2,[26-28] with a $4f^0$ electronic configuration and displaying one of the most complex spectra observed in x-ray photoelectron spectroscopy.

3.4. Multiplet Splitting

One of the consequences of paramagnetic metal ions in x-ray photoelectron spectroscopy is that of multiplet splitting. In the case of transition metal ion systems, this has been studied extensively. The principles of multiplet splitting for this group of metal species are well understood, and the effects on their x-ray photoelectron spectra have been documented for a large number of compounds. The subtle differences among the spectra as a function of chemical species make the phenomenon of multiplet splitting extremely useful.

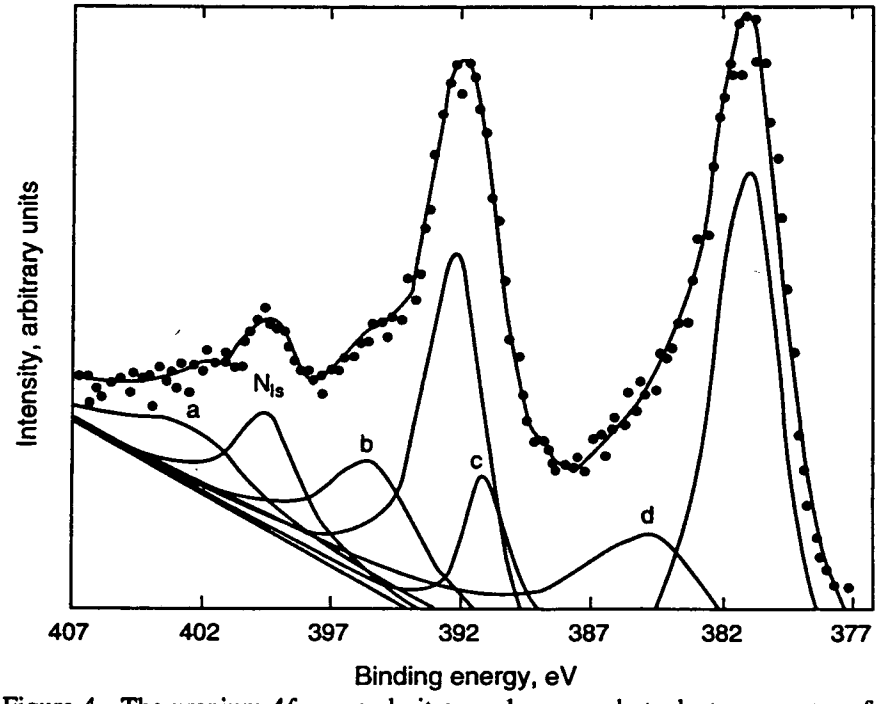

Figure 4. The uranium $4f_{7/2,5/2}$ and nitrogen $1s$ x-ray photoelectron spectra of the complex $[(C_2H_5)_2NH_2]^+$ $[UO_2((C_2H_5)_2NCOS)_2$ $OC_2H_5]^-$. Adapted from Reference 24. (XBL 918-6098)

Multiplet splitting results from interactions among electrons in core and valence electronic shells. In diamagnetic, electron closed shell configuration ions, only one final electronic state is usually formed. Paramagnetic metal ions such as are found in the $3d$ transition series, however, present a different case as a result of the ejection of the electron in the photoelectron process. Since there are unpaired electrons in the valence shell of many of these ions, several electronic states can result when a vacancy is effected in an inner shell. This occurs because the ejected electron causes exchange interactions that will affect the spin-up and spin-down electrons differently. Two final states will occur if the ejected electron is from an s level in a paramagnetic species. If the investigator is observing the $3s$ level in paramagnetic transition metal ions such as Mn^{2+}, Fe^{3+} or Cr^{3+}, the splitting will be dependent on the exchange integral between the $3d$ and $3s$ orbitals. Theoretical calculations, taking into account covalency parameters, have been made for a number of transition metal species, and these calculations have been found to be in varying agreement with experimental results. The splitting, of course, varies as a function of the types of ligands around the central ion.

The effects of multiplet splitting manifest themselves in both quite subtle and dramatic ways, depending on the portion of the x-ray photoelectron spectrum being studied. Perhaps the most widely observed core levels reported for the $3d$ transition metals is the $2p$ level. In their spectra, the $2p$ lines broaden as a result of multiplet splitting. More significantly, however, the $3s$ level is changed quite dramatically, being split into a doublet spectrum. Each paramagnetic species exhibits a unique splitting magnitude.

Taking note of the effects of multiplet splitting on x-ray photoelectron spectra, then, an investigator can many times differentiate among several different inorganic materials. In Figure 5, the $3s$ x-ray photoelectron spectra taken using Al Kα x-rays for several transition metal compounds of varying electronic states and structures.[29] Chromium(III) fluoride exhibits a $3d^3$ valence shell configuration with all three d electrons unpaired; the resulting multiplet splitting is 4.2 eV. Manganese(II) fluoride possesses a high-spin $3d^5$, paramagnetic configuration, showing a splitting of 6.3 eV. In addition to this observation concerning the $3s$ level, the $2p_{1/2}$ photoelectron peaks of this compound exhibit broadening. Gupta and Sen[30] have carried out calculations that take into account crystal field effects, electronic configuration interactions, and spin-orbit splitting. While multiplet splitting does indeed effect the formation of several final electronic states, this broadening of the $2p$ lines and the lack of well defined satellite structure associated with them are the main consequences in the $2p$ level. Experimental data[31] verify these calculations.

The last two compounds in Figure 5 represent an interesting contrast for two iron(II) compounds with a $3d^6$ valence shell configuration. FeF_2 is a high-spin paramagnetic compound showing a multiplet splitting of 6.0 eV for the $3s$ shell. The complex $K_4\ Fe(CN)_6$, however, while also a $3d^6$ valence shell, is a case in which the iron(II) is surrounded by six strong-field cyano ligands. Thus, the iron(II) in this compound is in a low-spin $3d^6$ spin state, in which all six electrons are paired. The resulting compound is thus diamagnetic and shows no multiplet splitting of the $3s$ level.

Similar splittings of the $3s$ level of the chromium(III) species can be observed in Figure 6. However, one anomaly can be seen in the last compound, $K_3\ Cr(CN)_6$. If chromium(III) is a paramagnetic species (and indeed it must be, since there is no way of pairing three d electrons), why is no multiplet splitting observed? Not even the strong-field cyano ligand alter the three unpaired electrons. A reasonable explanation is that the valence $3d$ electrons undergo a substantial amount of delocalization.[29] This occurs because of π backbonding between the empty CN^- antibonding π-orbital and the chromium non-bonding t_{2g} orbital. This results in a metal-to-ligand $Cr(t_{2g}) \rightarrow CN^-\ (\pi^*)$ electron transfer and no multiplet splitting.

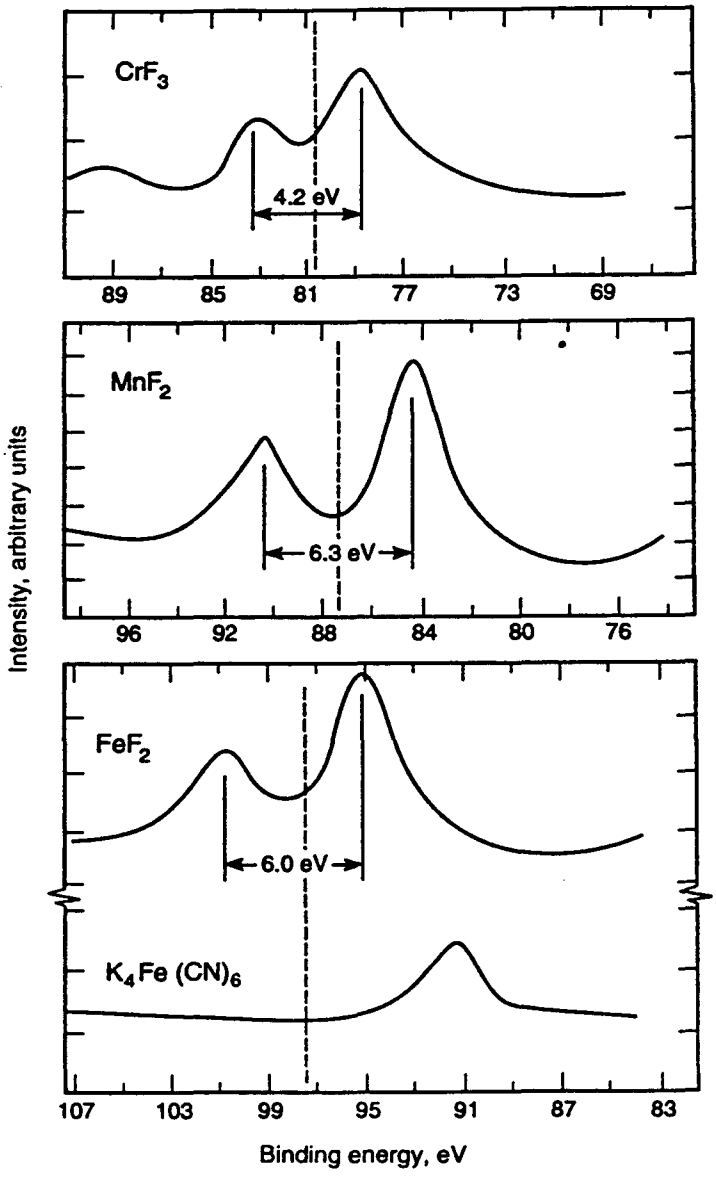

Figure 5. The 3*s* x-ray photoelectron spectra for CrF_3, MnF_2, FeF_2, and $K_4Fe(CN)_6$. Adapted from Reference 29. (XBL 911-6424)

3.5. Auger Parameters

In using the combined x-ray photoelectron/Auger spectrum to study different inorganic materials, one of the most powerful concepts is that of the Auger parameter. From Figure 1, it is noted that both the x-ray photoelectron and Auger events occur approximately simultaneously in the combined spectrum of a material, and both are readily observed. As noted above, the Auger shifts can many times be much greater than the binding energy shifts. Using both spectral features, then, gives an investigator an inherent advantage in not having to rely solely on either. Thus, it is advantageous to have a quantitative experimental parameter that reflects the chemical state of a material species referenced to an element in that species.

The Auger parameter[9,10] is an effective approach that describes the chemical and electronic states of such species. The basis of the concept is explained using two approaches. First, in noting that the Auger shifts greatly exceed the x-ray photoelectron binding energy shifts for several elements, it is observed that this phenomenon occurs if two criteria are met: these criteria are that a) the initial vacancy is in an inner shell, and b)

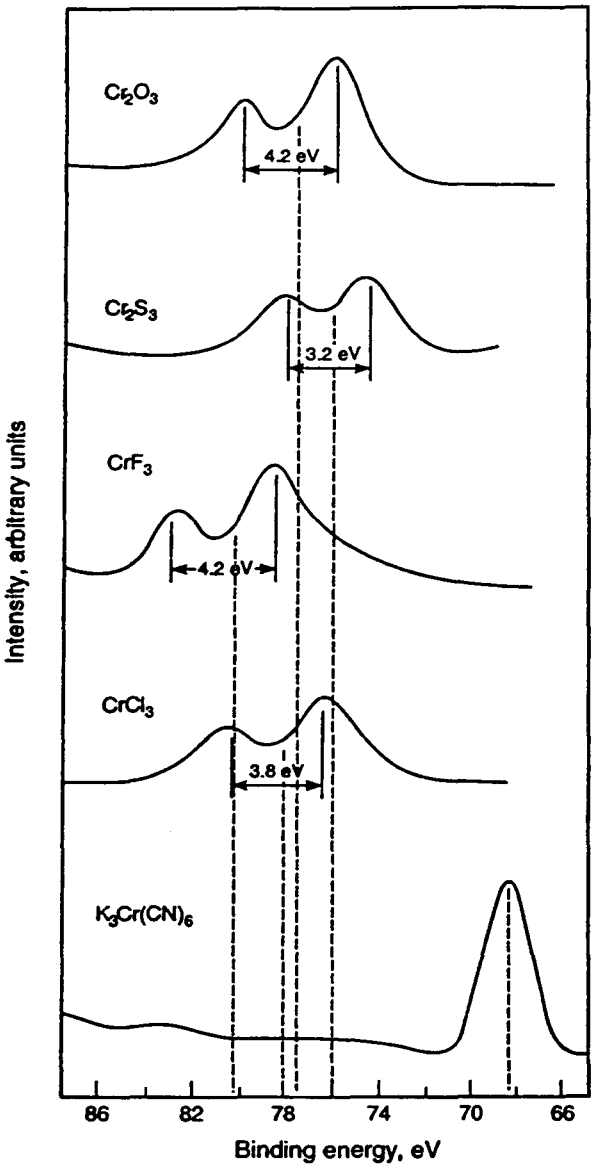

Figure 6. The 3*s* x-ray photoelectron spectra for several chromium(III) compounds obtained using Al Ka radiation. Adapted from Reference 29. (XBL 911-6425)

the element under study is a conductor. The differences, then, in the polarization energy thus provide one factor in the differences between Auger and photoelectron chemical shifts. This is not surprising in light of the fact that the Auger emission results in a doubly ionized final state, while the photoemission event results in only a single ionized state.

A second approach to explaining the Auger parameter is rooted in the concept of extra-atomic relaxation.[32,33] This approach combines Hartree-Fock orbital energies and relaxation effects on the Auger energies. The extra-atomic relaxation is a result of the polarization of adjacent molecules in a material.

Briefly, an abridged derivation for the Auger parameter for the nitrogen *1s* photoelectron and the nitrogen *KVV* Auger electron is as follows.[9,10] When comparing the large Auger chemical shift relative to that of the photoelectron shift, the larger Auger shift will obviously be a major component of the combined shifts, or the Auger parameter. Both shifts must be determined, however, in order to obtain the parameter. In going from the

state of an isolated atom to an elemental, conductive state, the photoelectron shift in kinetic energy can be described in Equation 2 as

$$\Delta KE\ (PE_{i\rightarrow e}) = -\Delta e_e + R_e^{ei} \tag{2}$$

while the kinetic energy shift of the Auger electron is in Equation 3.

$$\Delta KE\ (A_{i\rightarrow e}) = -\Delta \varepsilon_e + R_e^{ei}\,(K^+) \tag{3}$$

In these two equations, $\Delta\varepsilon_e$ is the electron shell energy in the ground elemental conductive state, e, and R_e^{ei} is the extra-atomic polarization (or relaxation) energy for the single hole K^+ atom. Subtracting the photoelectron kinetic energy from the Auger kinetic energy yields the change in the Auger parameter

$$\Delta\alpha_{i\rightarrow e} = 2R_e^{ei}\,(K^+) \tag{4}$$

for a one-hole state and

$$\Delta\alpha_{i\rightarrow e} = 0.5\ R_e^{ei}\,(V^+V^+) \tag{5}$$

for a two-hole state.

The modified Auger parameter,[9,10] making use of Wagner's definition (Eqn. 6)

$$\alpha = E_{Auger} - E_{photoelectron} \tag{6}$$

takes into account the energy relationship

$$E_{photoelectron} = h\upsilon - E_{photoelectron\ binding\ energy} \tag{7}$$

Thus, the final modified Auger parameter (α_w) form that is frequently used takes the form shown in Equation 8.

$$\alpha_w = \alpha + h\upsilon = E_{Auger} + E_{photoelectron\ binding\ energy} \tag{8}$$

In practice, one can take the Auger line expressed as a binding energy as shown in Figure 2 and subtract it from the excitation (anode) energy, hυ, in order to obtain the kinetic energy for the Auger electron, E_{Auger}. For the Auger parameter for nitrogen for BN, the kinetic energy for the nitrogen *KVV* Auger line would be the value of hυ, 1253.6 eV, minus the nitrogen *KVV* line in the spectrum expressed as a binding energy (873.4 eV), yielding 380.2 eV. When the Auger kinetic energy is added to the binding energy of the nitrogen 1*s* photoelectron line, 397.9 eV, the sum, 778.1 eV, is the modified Auger parameter, α_w, for nitrogen in boron nitride, BN.

A second example can be seen in Figure 7 for the case of gallium arsenide, GaAs, an important semiconductor material. Using the sharpest, most-intense, and best-resolved Auger line, $L_3M_{45}M_{45}$, its value expressed as a binding energy, 261.0 eV is subtracted from the value of hυ, 1486.6 eV, for the Al *Kα* radiation of the anode; this results in a value of 1225.6 eV for the As $L_3M_{45}M_{45}$ kinetic energy. Adding 1225.6 eV to the arsenic $3d_{5/2,3/2}$ photoelectron line binding energy (in this case, the $d_{5/2}$ and $d_{3/2}$ lines are so close, ~ 1 eV, they are unresolved and appear as a single line) of 40.7 eV gives 1266.3 eV for the Auger parameter of arsenic in GaAs.

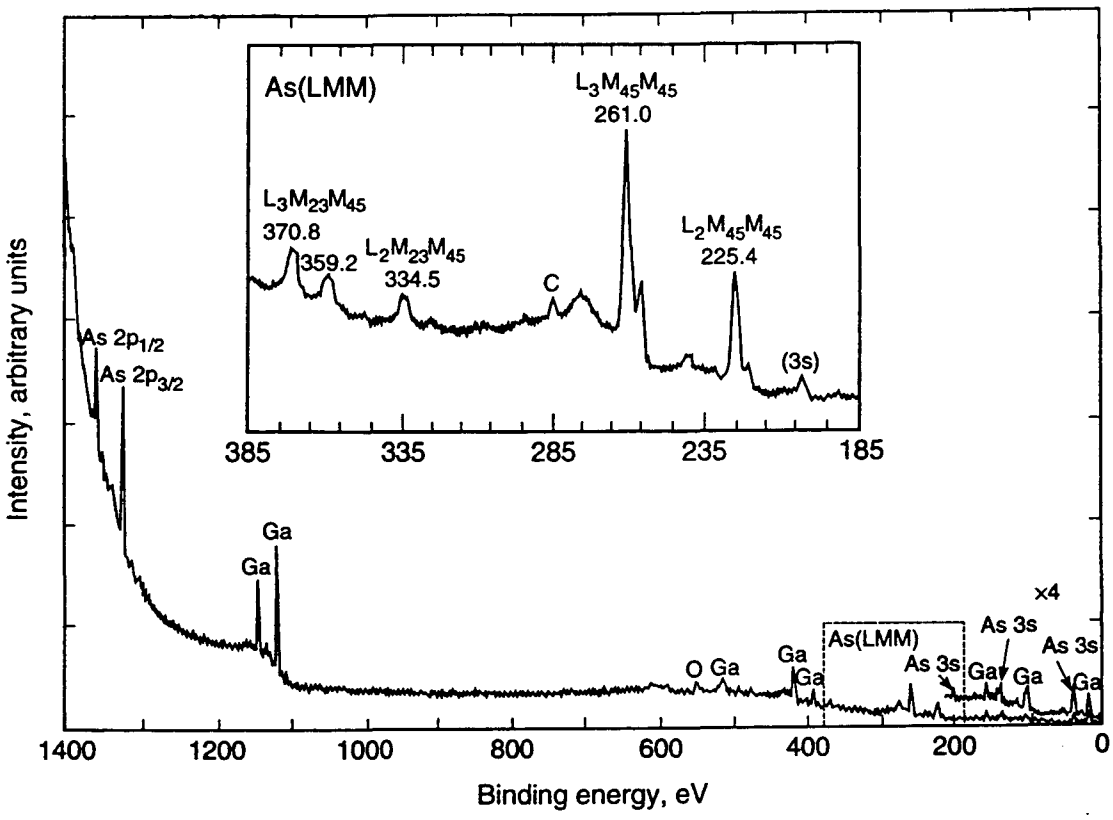

Figure 7. Survey scan of the combined x-ray photoelectron and Auger spectra of gallium arsenide, GaAs, using Al *Ka* radiation. Adapted from Reference 9. (XBL 911-6423)

Use of the Auger parameter in studying the chemical state of an element in a material has several decided advantages. First, both spectral lines are contained in the same combined spectrum and are thus "internally calibrated," i.e., they are at fixed locations relative to one another. Second, charge corrections are unnecessary due to this internal calibration; this is especially useful in the study of insulating materials. Finally, again, because of both spectra being combined, there is no need to evaluate the work function in Equation 1 for a spectrometer, and Fermi level and vacuum level data can be compared directly.

Table 2 contains selected materials and their Auger parameters that have been reported in the literature. The compilation is by no means comprehensive, but it is intended to give some picture of the variations among the photoelectron and Auger lines and the resulting Auger parameters as a function of widely different chemical species and electronic states. In each case the materials are compared to the parent element itself in order to show the degree of shift across several diverse chemical types of compounds.

The reader should note that in some cases, the differences among compounds for a particular element may vary greatly or almost not at all. In the case of selenium, for example, selenium has a range of over 6 eV and 8 eV for its photoelectron and $L_3M_{45}M_{45}$ Auger lines, respectively, for elemental selenium and Na_2SeO_4; its Auger parameter varies by only about 3 eV. Titanium, however, while varying by ~8.5 eV in its photoelectron line and ~9 eV for its $L_3M_{23}M_{23}$ Auger line for the entries in Table 2, has an Auger parameter that exhibits a difference of less than a volt. Clearly, an investigator must make judicious comparisons among not only one line of an element in a series of compounds, but of several. Indeed, sometimes minor lines also may have to be studied, along with other spectral features such as the spin-orbit splitting and satellite structure outlined above.

Table 2. Representative Inorganic Materials and Their Auger Parameters[a]

Compound	Photoelectron Line	Auger Line	Auger Parameter,	Ref.
Aluminum	***2p***	***$KL_{23}L_{23}$***		
Al°	72.9	1393.3	1466.2	[79]
AlAs	73.6	1391.2	1464.8	[79]
α-Al_2O_3	73.8	1388.2	1462.0	[78]
AlOOH (Boehmite)	74.2	1387.6	1461.8	[78]
Molecular Sieve-A	73.7	1386.9	1460.6	[78]
Gallium	***3d***	***$L_3M_{45}M_{45}$***		
Ga°	18.5	1068.1	1086.6	[110]
GaAs (Cleaved)	19.4	1066.2	1085.6	[110]
GaN	19.5	1064.5	1084.0	[111]
Ga_2O_3	21.0	1061.9	1082.9	[110]
Germanium	***3d***	***$L_3M_{45}M_{45}$***		
Ge°	29.0	1145.4	1174.4	[112]
GeS_2	30.5	1143.7	1174.2	[112]
GeO_2	32.7	1137.7	1170.4	[113]
Na_2GeF_6	33.3	1135.7	1169.0	[113]
Iron	***$2p_{3/2}$***	***L_3VV***		
Fe°	707.0	702.4	1409.4	[9]
FeS_2	707.4	702.7	1410.1	[36]
$FeSO_4 \cdot 7H_2O$	711.0	700.4	1411.4	[36]
$K_3Fe(CN)_6$	709.9	698.4	1408.3	[36]
Lead	***$4f_{7/2}$***	***$N_6O_{45}O_{45}$***		
Pb°	136.7	95.9	232.6	[15]
PbO_2	137.3	92.7	230.0	[15]
$Pb(OH)_2$	138.0	91.6	229.6	[15]
PbF_2	138.5	90.6	229.1	[114]
$PbWO_4$	138.7	91.8	230.5	[114]
Palladium	***$3d_{5/2}$***	***$M_4N_4N_{45}$***		
Pd°	335.1	327.8	662.9	[9]
$PdSO_4$	338.7	324.8	663.5	[36]
$Pd(NO_3)_2$	338.2	324.7	662.9	[36]
$PdCl_2$	338.0	325.2	662.2	[36]
Na_2PdCl_4	338.0	323.4	661.4	[36]
Selenium	***$3d_{5/2}$***	***$L_3M_{45}M_{45}$***		
Se°	55.5	1307.0	1362.5	[115]
SeO_2	59.0	1301.4	1360.4	[115]
Na_2SeO_3	58.5	1301.2	1359.7	[36]
Na_2SeO_4	60.6	1298.9	1359.5	[36]
Silicon	***2p***	***$KL_{23}L_{23}$***		
Si°	99.4	1616.7	1716.1	78]
Si_3N_4	101.9	1612.2	1714.1	[84]
SiO_2(Quartz)	103.6	1608.6	1712.2	[82]
SiO_2(Gel)	103.6	1607.9	1711.5	[82]
$MoSi_2$	99.6	1617.2	1716.8	[78]

Table 3. Inorganic Materials Studied by X-Ray Photoelectron and Combined X-Ray Photoelectron/Auger Spectroscopy

Material	Compounds Studied	References
Actinides	Oxides and fluorides of the *5f* elements actinium through einsteinium.	[21]
Aluminates	$NiAl_2O_4$	[96]
Arsenides	NbAs	[97]
Borates	$Na_3B_3O_6$, H_3BO_3, $Na_2B_4O_7 \cdot 10H_2O$	[40]
Borides	Fe_2B, VB_2, CoB, HfB_2, AlB_2	[98]
Carbides	WC, HfC, TiC	[99]
Carbonates	$NaHCO_3$ Na_2CO_3	[41]
(per-)Chlorates	$KClO_4$, $KClO_3$	[34]
Chromates (-ites)	Li $_2CrO_4$, $LiCrO_2$, $Na_2Cr_2O_7$	[100]
Ferrates (-ites)	$NiFe_2O_4$	[101]
Germanates	Na_2GeO_3	[102]
Halides		
Bromides	Simple salts, complexes	[45]
Chlorides		[45]
Fluorides		[45]
Iodides		[45]
Inorganic Complexes	Coordination and chelate complexes	[47]
Lanthanides	Oxides	[70]
Molybdates	$CoMoO_4$, $Al_2(MoO_4)_3$	[103]
Nitrates (-ites)	$NaNO_3$, NH_4NO_3, $NaNO_2$	[42]
Niobates	$KNbO_3$	[68]
Nitrides	WN	[104]
Phosphates	Na_3PO_4, $Na_4P_2O_7$, Li_3PO_4, $Li_4P_2O_7$	[105]
Phosphazenes	$(NPR_2)_n$	[90]
Selenates(-ites)	Na_2SeO_4, Na_2SeO_3	[43]
Phosphides	BP, MnP, CrP	[106]
Selenides	SnSe, PbSe, As_2Se_3	[43]
Silicates	SiO_2 and derivatives	[82]
Silicides	$MoSi_2$	[78]
Sulfates(-ites)	$FeSO_4$, Na_2SO_4, Na_2SO_3	[44]
Sulfides	$KFeS_2$, FeS	[107]
Titanates	$BaTiO_3$, $PbTiO_3$	[108]
Tungstates	$Al_2(WO_4)_3$, $NiWO_4$	[109]

4. APPLICATIONS

As is obvious from the different types of electronic information discussed above that one can derive using x-ray photoelectron and Auger spectroscopy, there is an extremely wide variety of inorganic materials that can be studied. An attempt is made below to discuss briefly as wide a range of examples as possible, including simple salts, oxides, inorganic complexes, and materials that have a lot of applications in materials science; these include such inorganics as superconductors, catalysts, and inorganic polymers. Although Table 3 contains a wide array of inorganic materials, several of them are discussed in greater detail below. The author has tried to balance the treatment of inor-

Table 2. Representative Inorganic Materials and Their Auger Parameters.[a] (Continued)

Compound	Photoelectron Line	Auger Line	Auger Parameter,	Ref.
Titanium	$2p_{3/2}$	$L_3M_{23}M_{23}$		
Ti°	454.0	419.1	873.1	[9]
TiC	454.6	418.2	872.8	[36]
TiN	455.7	420.0	875.7	[36]
TiO_2	458.5	414.7	873.2	[36]
Na_2TiF_6	462.6	409.8	872.4	[36]

[a]Partially abstracted from Reference 65. The photoelectron and Auger lines (and thus their Auger parameters) have been corrected for charging in Reference 65, using standard values for the gold, copper, and carbon lines. The reader should see the original references for complete experimental details on each compound.

ganic compounds and inorganic materials, keeping in mind that any elemental bonding approach studies of inorganic compounds are directly applicable to any materials involving those same elements.

4.1. Inorganic Salts

There are many studies in the literature dealing with inorganic salts. In many cases the x-ray photoelectron and Auger data can be used to differentiate among different salts involving the same element, much the same way as the ammonium and nitrate salts discussed above can be distinguished from one another with respect to their nitrogen oxidation states. The above example involving the high binding energy of the sulfur $2p$ photoelectron line in the sulfate salt is another case. Other systems of salts that can be distinguished using either x-ray photoelectron and/or x-ray -induced photoelectron and Auger spectroscopy in conjunction with Auger parameters are chloride-perchlorates,[34] bromide-bromates,[35] iodide-iodates,[36] and telluride-tellurates.[37] Auger parameters have also been reported for phosphates,[38,39] while x-ray photoelectron data are in the literature for borates,[40] carbonates,[41] nitrates,[42] selenates,[43] and sulfates.[44]

In some instances x-ray photoelectron and Auger spectroscopy can be used to give definitive structural information about a salt rather than just its chemical and electronic state. Walton[45] has shown that the chlorine $2p_{3/2,1/2}$ doublet can be used to distinguish between terminal and bridging chloride species. In Figure 8, for example, the chlorine $2p_{3/2,1/2}$ spectra for two chloro-containing complexes have been resoluted, showing both bridging and terminal chloride species. The binding energy for the spin-orbit doublet assigned to bridging chlorides is ~1.5 eV greater than that of the binding energy for that of the terminal chlorides. The bridging:terminal chloride intensity ratio is 2:1, in good agreement with crystal structure data for Re_3Cl_9 and its derivatives. Similarly, the $Re_3Cl_6(acac)_3$ complex exhibited a chlorine $2p_{3/2,1/2}$ spectrum with an intensity ratio of 1:1 for the bridging vs. terminal chlorides, again in agreement with known structures.

In addition to being able to identify different chemical states of an element in different salts, the Auger parameter has been shown to be quite effective in the differentiation of many inorganic salts from other compounds of a particular element. One of the best examples of this is that of cadmium and several of its compounds[46] as shown in Figure 9. While the difference in the binding energies of the $3d_{5/2}$ level for CdO and CdF_2 is a fairly substantial 1.7 eV, the kinetic energy difference for the $M_{45}N_{45}N_{45}$ level for the

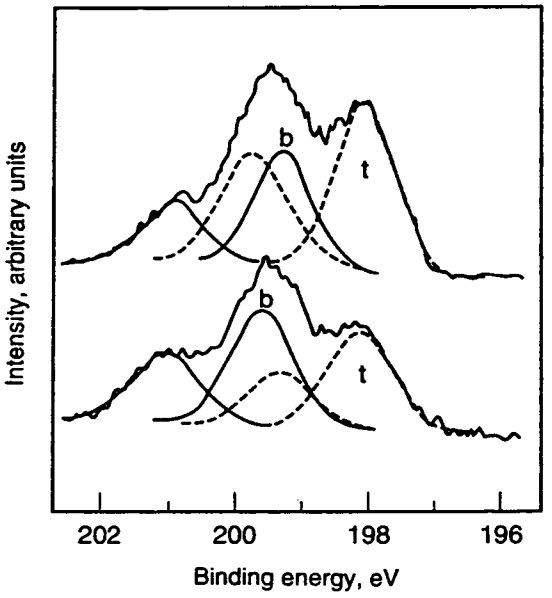

Figure 8. The curve resolved chlorine $2p_{3/2,1/2}$ x-ray photoelectron spectra of $Re_3Cl_9(pyz)_3$ (pyz = pyrazine) (top) and $Re_3Cl_6(acac)_3$ (acac = acetylacetone) (bottom) indicating bridging and terminal chlorides. Adapted from Reference 45. (XBL 911-6422)

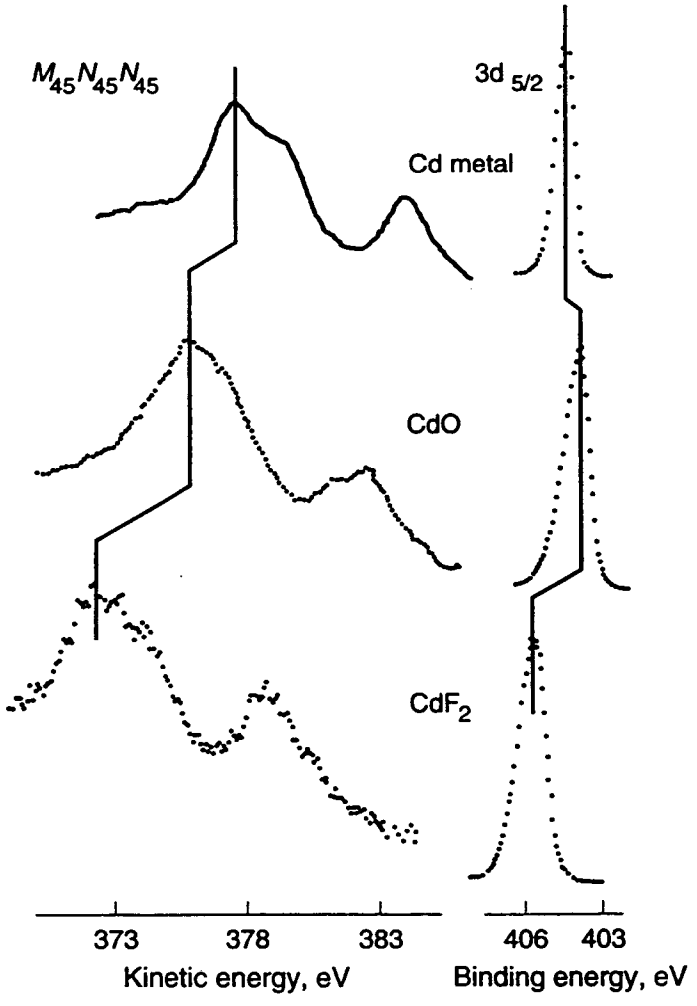

Figure 9. The x-ray photoelectron and Auger spectra of selected cadmium compounds. Adapted from Reference 46. (XBL 918-6100)

two compounds is a very substantial 3.4 eV; thus, the resulting Auger parameters for the two compounds are also quite different and can be readily used to distinguish between the compounds.

4.2. Inorganic Complexes

One of the most fruitful areas of study for the application of x-ray photoelectron and Auger spectroscopy is that of solid inorganic complexes. In addition to the bridging and terminal chloride structural determinations discussed above, an investigator can use spectral characteristics such as multiplet-splitting and satellite structure to get a detailed picture of the bonding and chemistry of the central element and the complexing ligands attached to it. A wide variety of complexes has been studied, and a few illustrative examples are presented here. The reader is also referred to an extensive review of metal complexes that have been studied by x-ray photoelectron spectroscopy.[47]

Meisel and co-workers[48] have applied extended Hückel theory and x-ray photoelectron spectroscopy to the study of several nickel(II) complexes, including $Ni(PH_3)_2Cl_2$, $Ni(NH_2CSNCOH)_2$, and $Ni[(CH_3O)_2\ PS_2]_2$. Other inorganic salts, along with their shake-up satellites, that were studied included the nickel(II) acetate, nitrate, chloride, and sulfate.

X-ray photoelectron studies have been conducted[49] on the series of transition metal dithiolate complexes $R_n^+[M(X)_2]^{n-}$ where n = 1 and 2 and M = Co(II), Co(III), Ni(II), Ni(III), Cu(II), Pd(II), and Pt(II). The ligands X are the dithiolate derivatives maleonitriledithiolate, dithiosquarate, dithiocrocanate, and dicyanomethylenedithiocrocanate, while the countercations (R^+) were alkylammonium salts. Other systems of this type that have been studied include the iron dithiolates.[50]

Roe and co-workers[51] have studied a series of octahedral copper(II) diamine tetrafluoroborate and perchlorate complexes from several standpoints. These include the degree of cation-anion interaction, the inductive effects of the diamine substituents, the Jahn-Teller effect, and the effects of altering the diamine chelate ring size.

X-ray photoelectron spectroscopy has been quite useful in determining the protonated vs. unprotonated forms of ethylenediaminetetraacetic acid (EDTA) in its complexes with metals.[52] In the formation of such complexes, the charge on the nitrogen atoms in EDTA has been shown to be substantially different depending on whether they are protonated. The binding energies of the nitrogen 1*s* line, therefore, are also quite different; the unprotonated form has a binding energy of ~ 398 eV, while the protonated form exhibits an energy of ~ 400 eV or more. Figure 10 shows the results for several complexed and uncomplexed salts. In the case of one protonated EDTA reagent salt, H_4EDTA, for example, the nitrogen 1*s* line has a value of 402.2 eV; the Mg_2EDTA complex, however, exhibits a value of 399.8 eV. One complex, MgH_2EDTA, apparently contains both forms, since a doublet is observed with binding energies at 399.8 and 402.2 eV.

4.3. Superconducting Metal Oxides

Perhaps no other group of inorganic materials has made a bigger impact on the field of materials sciences in recent years than that of the superconducting metal oxides.[53] While there are many metal oxide derivatives now in the literature, many contain the barium-lanthanum-copper oxide core; still many others consist of this same core but with other metals present as either major components or as dopants. Several reports of x-ray photoelectron and Auger studies of these superconductors have appeared, the studies dealing with both the bulk and surface properties using these techniques. Kohiki and coworkers[54] have studied the $YBa_2Cu_3O_7$ superconducting compound, with attention being

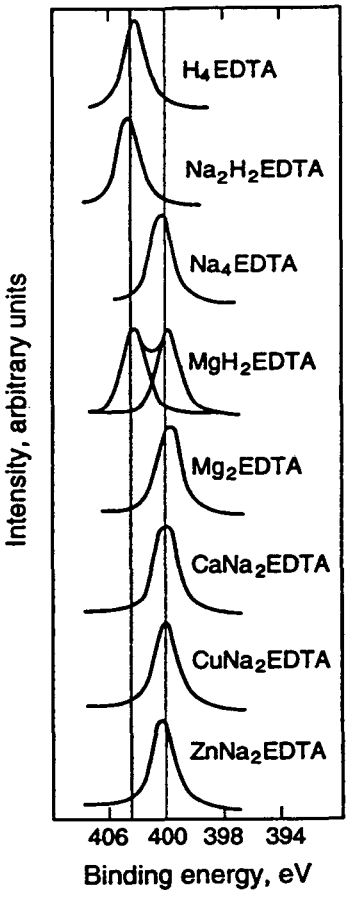

Figure 10. The nitrogen 1*s* x-ray photoelectron spectra of EDTA and several complexes. Adapted from Reference 52. (XBL 918-6097)

paid to the temperature-dependent copper-oxygen bond basal plane atoms. It was found that the intensity of the oxygen 1*s* photoelectron line attributed to the copper-oxygen bond decreased with decreasing temperature. The valence band spectra at varying temperatures contained one major component attributed to strong interaction between the copper 3*d* electrons and the neighboring 2*p* electrons with x^2 - y^2 symmetry in the *x-y* plane. The copper $2p_{3/2}$ and barium $3d_{5/2}$ spectra were also studied as a function of varying temperature.

Another group of researchers[55] addressed the issue of the synthesis process of the $YBa_2Cu_3O_{7-y}$ phase and its contaminants using x-ray photoelectron and Auger spectroscopy. The carbon 1*s* photoelectron and *KVV* Auger spectra showed carboxylate contamination to be present in the final solid material. The carboxylate/carbonate most likely originated from the incomplete $BaCO_3$ synthesis precursor; argon ion sputtering-induced depth profiling showed the carbonate species to be present to a depth of approximately 150 Å into the solid bulk.

Other researchers[56] have studied the various aspects of the superconducting metal oxides surfaces and their interactions with various agents such as air, carbon dioxide, and water; the superconducting phases investigated were $YBa_2Cu_3O_x$ and $Bi_2Sr_2CaCu_2O_x$. In $YBa_2Cu_3O_x$ the surface was found to be enriched with barium and depleted with respect

to copper, the reason presumably being due to the formation of $BaCO_3$ and/or $Ba(OH)_2$ formed by atmospheric reaction. Annealing in moist oxygen led to a Y_2BaCuO_5 surface phase (which dropped in its superconducting capability), while annealing of the bismuth-based material in moist oxygen resulted in no substantial changes in the surface layer compositions.

Interfaces between superconducting metal oxides and various substrates have also been studied.[57,58] In one study nickel films were condensed onto two different superconducting materials, $YBa_2Cu_3O_{7-x}$ (A) and $Bi_2Sr_2Ca_{0.8}Y_{0.2}Cu_2O_x$ (B).[59] In the initial stage of deposition of the nickel film on (A), one sees (at a depth of 0.5 Å) a doublet feature for the nickel $2p_{3/2}$ line in Figure 11. A nickel oxide bulk-type line is observed at ~ 855 eV, with the shift from the reported 854.5 eV of NiO presumably due to differences between bulk NiO and the local interface-induced NiO environment. As the nickel film becomes thicker, the spectrum takes on the complete features of metallic nickel and its shake-up satellite 6 eV to the higher binding energy side of the main line at 852.7 eV.

In addition to the superconducting oxides themselves, many studies have also been reported on the component elements and their oxides. Copper, for example, and its oxides and salts have been the object of several investigations by many different workers. In the case of copper, perhaps the most common and prevalent ion in superconducting metal oxides, several studies reporting the x-ray photoelectron and Auger data for its compounds have been published.[60-64] The Auger parameters for compounds of copper have also been published.[10,65] X-ray photoelectron data are also found in the literature for bismuth,[66-67] thallium,[68] calcium,[65,69] and many rare earths such as cerium,[26-28] praseodymium,[70] terbium,[70,71] gadolinium,[70,72] europium,[73] ytterbium,[70] and lanthanum.[74-76]

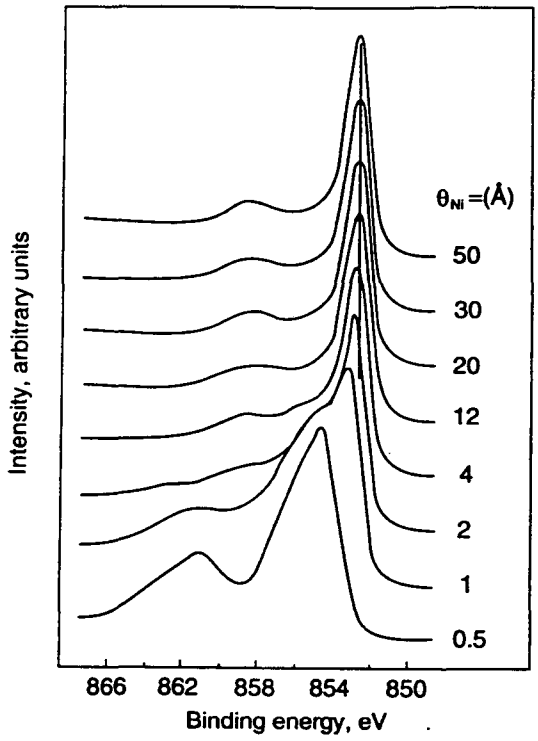

Figure 11. The nickel $2p_{3/2}$ x-ray photoelectron spectra of nickel deposited on $YBa_2Cu_3O_{7-x}$. Adapted from Reference 59. (XBL 918-6101)

4.4. Catalytic Supports and Precursors

X-ray photoelectron and Auger spectroscopy provide excellent experimental approaches to the study of catalysts, since researchers are interested in both the chemistry of the catalysts and the interfacial surface reactions they undergo in the catalysis process. The extraordinary number of studies in the literature in this field places any attempt at an extensive discussion of it beyond the scope of this work; the chemistries of the individual catalytic species are also covered in the research literature under their parent elements. However, mention is made below of several studies reported in the literature related to catalytic supports that are frequently used, a group of materials that is considerably smaller than the catalysts themselves. Two of these that are commonly used are alumina and silica,[77] two of the most widely studied oxides using x-ray photoelectron and Auger spectroscopy.

Aluminum, its oxide and hydroxides in various forms, and oxide-hydroxides have been the subjects of dozens of studies. Aluminum and its oxidation has been studied by various investigators,[78-81] while other studies have centered on the various forms of the bulk oxide such as α- and γ-Al_2O_3.[78] Alumina-precursor hydroxides of the type $Al(OH)_3$ (bayerite[79,82] and gibbsite[78]) appear in the literature, as does the goethite aluminum analog compound of the formula AlO(OH), boehmite.[78] The Auger parameters and their chemical state plots of the above aluminum compounds and related ones have been published.[10,37] Molecular sieves and their Auger parameters have also been recorded.[78]

Silicon dioxide and related compounds have also been extensively studied. Silica gel has been investigated by a number of groups.[35,82-83] As is the case with the aluminum-alumina system above, studies of the oxidation of silicon leading to the formation of silicon oxides are in the literature.[78,84] Research has also been conducted on quartz,[35,85] vapor deposited SiO_2,[86] and cristobalite.[78] Work on zeolites and other aluminosilicates[87-89] that are used as catalytic supports has also been reported.

4.5. Inorganic Polymers

While many people think of only organic base units when the word "polymer" is mentioned, there is a fairly substantially large number of *inorganic* polymers in the chemical literature. Several spectroscopic studies of these different types of materials that are pertinent to the present treatise are briefly discussed below.

Polyphosphazenes, inorganic polymers of the type $[NPR_2]_n$, consist of alternating nitrogen and phosphorus backbones. X-ray photoelectron and Auger spectroscopy studies[90] centered around the phosphorus photoelectron line and x-ray excited Auger line and their shifts relative to the electronegativity and polarizability of the side groups attached to the phosphorus atoms. The phosphorus Auger parameter for the polymers was found to always be higher than that of the corresponding trimers; for the cases studied, the R groups were the chloride, fluoride, methoxy, trifluoroethoxy, and phenoxy species. Additionally, the nitrogen 1*s* and Auger *KVV* line-based Auger parameters for the phosphazenes were reported.

Another polymer system with an inorganic base that has been studied with x-ray photoelectron spectroscopy is that of polyphenylacetylene (PPA)-polyiodide films.[91] The iodine $3d_{5/2}$ core level spectra were used to follow the formation of the films that resulted from the interaction of the PPA-reacting substrate with iodine vapor under various experimental conditions, primarily a variation in the reaction time. The x-ray photoelectron data were consistent with the formation of the I_5^- species doped into the PPA starting film; this resulting PPA-I_5^- complex was found to be stable under ultra high vacuum at temperatures up to 250 °C. By making use of the iodine $3d_{3/2}/3p_{3/2}$ intensity ratio, the authors were able to ascertain that the iodine species resided in the near-surface region of

the PPA organic film. This finding was consistent with results published for other similar iodine-polymer interaction products. X-ray photoelectron studies have also been published for other I_2-doped polymers.[92-94]

X-ray photoelectron and x-ray induced Auger spectroscopy has been used to study organic films on metals and alloys. Surface films of benzotriazole (BTA) on zinc and copper-zinc alloys have been reported.[95] X-ray photoelectron spectroscopy by itself could not distinguish between metallic copper and copper(I); however, with the additional use of the copper *LMM* and zinc *LMM* Auger lines, it was possible to clearly obtain a knowledge of the two states. Two different chemical species were formed in the surface films. In the case of the Zn-Cu alloys, the principal complex was shown to be copper(I)-BTA. A small amount of zinc(II)-BTA, however, was also identified as having been formed from the interaction.

Acknowledgments

The author wishes to acknowledge support of his research by the U.S. Department of Energy under Contract No. DE-AC03-76SF00098. Additional support has also been provided by the Assistant Secretary for Fossil Energy, Office of Oil, Gas, and Shale Technologies, through the Morgantown Energy Technology Center, Morgantown, West Virginia, and the Center for Science and Engineering Education, Lawrence Berkeley Laboratory, University of California.

References

1. P. Swift, *Surf. Interface Anal.*, 4, 47(1982).
2. J.Q. Broughton and D.L. Perry, *Surf. Sci.*, 74, 307(1978).
3. J.S. Brinen, *J. Electron Spectrosc. Relat. Phenom.*, 5, 377(1974).
4. J.C. Klein, C.P. Li, D.M. Hercules, and J.F. Black, *Appl. Spectros.*, 38, 729(1984).
5. B. Wallbank, C.E. Johnson, and I.G. Main, *J. Electron Spectrosc. Relat. Phenom.*, 4, 263(1974).
6. H. Yamada, K. Shriaishi, and N. Watanibe, *Nippon Kagaku Kaishi*, 8, 1245(1981).
7. C.R. Brundle, T.J. Chuang, and K. Wandelt, *Surf. Sci.*, 68, 459(1977).
8. K. Hirokawa and Y. Danzaki, *Surf. Interface Anal.*, 4, 63(1982).
9. C.D. Wagner, W.M. Riggs, and L.E. Davis, "Handbook of X-Ray Photoelectron Spectroscopy," Perkin-Elmer, Eden Prairie, MN(1979).
10. C.D. Wagner and A. Joshi, *J. Electron Spectrosc. Relat. Phenom.*, 47, 283(1988).
11. D. Briggs and M.P. Seah, Eds., "Practical Surface Analysis by Auger and X-Ray Photoelectron Spectroscopy," John Wiley & Sons, London(1983).
12. C.D. Wagner and P. Biloen, *Surf. Sci.*, 35, 82(1973).
13. D.C. Frost, A. Ishitani, and C.A. McDowell, *Mol. Phys.*, 24, 861(1972).
14. M.O. Krause and C.W. Nestor, *Phys. Scr.*, 16, 285(1977).
15. J.A. Taylor and D.L. Perry, *J. Vac. Sci. Technol. A*, 2, 771(1984).
16. M.A. Brisk and A.D. Baker, *J. Electron Spectrosc. Relat. Phenom.* 7, 197(1975).
17. L.J. Aarons, M.F. Guest, and I.H. Hillier, *J. Chem. Soc., Faraday Trans. II*, 68, 1866(1972).
18. A. Rosencwaig, G.K. Wertheim, and H.J. Guggenheim, *Phys. Rev. Lett.*, 27, 479(1971).
19. L.J. Matienzo, L.I. Yin, S.O. Grim, and W.E. Swartz, *Inorg. Chem.*, 12, 2762(1973).
20. G.A. Vernon, G. Stucky, and T.A. Carlson, *Inorg. Chem.*, 15, 278(1976).
21. M.O. Krause, R.G. Haire, O. Keski-Rahkonen, and J.R. Peterson, *J. Electron Spectrosc. Relat. Phenom.*, 47, 215(1988).

22. E. Thibaut, J.-P. Boutique, J.J. Verbist, J.-C. Levet, and H. Noel, *J. Am. Chem. Soc.*, 104, 5266(1982).
23. G.C. Allen, A.J. Griffiths, and B.J. Lee, *Transition Met. Chem.*, 3, 229(1978).
24. D.L. Perry, *Inorg. Chim. Acta*, 48, 117(1981).
25. J.J. Pireaux, J. Riga, C. Thibaut, C.T.-Noel, R. Caudano, and J.J. Verbist, *Chem. Phys.*, 22, 113(1977).
26. G. Praline, B.E. Koel, R.L. Hance, H.I. Lee, and J.M. White, *J. Electron Spectrosc. Relat. Phenom.*, 21, 17(1980).
27. G. Thornton and M.J. Dempsey, *Chem. Phys. Lett.*, 409(1981).
28. D.L. Perry, L. Tsao, and H.G. Brittain, *J. Mat. Sci. Lett.*, 3, 1017(1984).
29. J.C. Carver, G.K. Schweitzer, and T.A. Carlson, *J. Chem. Phys.*, 57, 973(1972).
30. R.P. Gupta and S.K. Sen, *Phys. Rev. B.*, 10, 71(1974).
31. S.P. Kowalczyk, L. Ley, F.R. McFeely, and D.A. Shirley, *Phys. Rev. B*, 11, 1721(1975).
32. D.A. Shirley, *Chem. Phys. Lett.*, 16, 220(1972).
33. D.A. Shirley, *Chem. Phys. Lett.*, 17, 312(1973).
34. V.I. Nefedov, A.K. Zhumadilov, and T.Y. Konitova, *J. Struct. Chem.*, 18, 692(1977).
35. C.D. Wagner, *J. Vac. Sci. Technol.*, 15, 518(1978).
36. C.D. Wagner, L.H. Gale, and R.H. Raymond, *Anal. Chem.*, 51, 466(1979).
37. C.D. Wagner *in* "Handbook of X-Ray and Ultra-Violet Photoelectron Spectroscopy," D. Briggs, Ed., Heyden & Sons, London(1977).
38. C.D. Wagner and J.A. Taylor, *J. Vac. Sci. Technol.*, 20, 83(1980).
39. A.J. Ashe, M.K. Bahl, K.D. Bomben, W.T. Chan, J. Gimzewski, P.A. Sitton, and T.D. Thomas, *J. Am. Chem. Soc.*, 101, 1764(1979).
40. D.N. Hendrickson, J.M. Hollander, and W.L. Jolly, *Inorg. Chem.*, 9, 612(1970).
41. U. Gelius, P.F. Heden, J. Hedman, B.J. Lindberg, R. Manne, R. Nordberg, C. Nordling, and K. Siegbahn, *Phys. Scr.*, 2, 70(1970).
42. B. Folkesson, *Acta Chem. Scand.*, 27, 287(1973).
43. U. Weser, G. Sokolowski, and W. Pilz, *J. Electron Spectrosc. Relat. Phenom.*, 10, 429(1977).
44. B.J. Lindberg, K. Hamrin, G. Johansson, U. Gelius, A. Fahlmann, C. Nordling, and K. Siegbahn, *Phys. Scr.*, 1, 277(1970).
45. R.A. Walton, *Coord. Chem. Rev.*, 21, 63(1976).
46. S.W. Gaarenstroom and N. Winograd, *J. Chem. Phys.*, 67, 3500(1977).
47. S. Srivastava, *Appl. Spectrosc. Rev.*, 22, 401(1986).
48. A. Meisel, R. Szargan, I. Uhlig, K.H. Hallmeier, J. Reinhold, and M. Casarin, *J. Electron Spectrosc. Relat. Phenom.*, 51, 459(1990).
49. S. Latitha and P.T. Monoharan, *J. Electron Spectrosc. Relat. Phenom.*, 49, 61(1989).
50. J. Blomquist, U. Helgesson, B. Folkesson, and R. Larsson, *Chem. Phys.*, 76, 71(1983).
51. S.P. Roe, J.O. Hill, and J. Liesegang, *J. Electron Spectrosc. Relat. Phenom.*, 46, 315(1988).
52. K.L. Cheng, J.C. Carver, and T.A. Carlson, *Inorg. Chem.*, 12, 1702(1973).
53. C.W. Chu, P.H. Hor, R.L. Meng, Z.J. Huang, and Y.Q. Wang, *Phys. Rev. Lett*, 58, 405(1987).
54. S. Kohiki, T. Hamada, and T. Wada, *Phys. Rev. B*, 36, 2290(1987).
55. F. Parmigiani, G. Chiarello, N. Ripamonti, H. Goretzki, and U. Roll, *Phys. Rev. B.*, 7148(1987).
56. V.I. Nefedov, A.N. Sokolov, M.A. Tyzykhov, N.N. Oleinikov, Y.A. Yeremina, and M.A. Kolotyrkina, *J. Electron Spectrosc. Relat. Phenon.*, 49, 47(1989).

57. P.A.P. Lindberg, Z.-X. Shen, W.E. Spicer, and I. Lindau, *Surf. Sci. Reports*, 11, 1(1990).
58. H.M. Meyer and J.H. Weaver, *in* "Physical Properties of High Temperature Superconductors II," D. M. Ginsberg, Ed., World Scientific, Inc. (1990), Chapter 6, p. 369.
59. H.M. Meyer, D.M. Hill, J.H. Weaver, K.C. Goretta, and U. Balachandran, *J. Mater. Res.*, 6, 270(1991).
60. D. Cahen, P.J. Ireland, L.L. Kazmerski, and F.A. Thiel, *J. Appl. Phys.*, 57, 4761(1985).
61. M.T. Anthony and M.P. Seah, *Surf. Interface Anal.*, 6, 95(1984).
62. R.J. Bird and P. Swift, *J. Electron Spectrosc. Relat. Phenom.*, 21, 227(1980).
63. B.R. Strohmeier, D.E. Leyden, R.S. Field, and D.M. Hercules, *J. Catal.*, 94, 514(1985).
64. J.C. Klein, A. Proctor, D.M. Hercules, and J.F. Black, *Anal. Chem.*, 55, 2055(1983).
65. C.D. Wagner, Auger and Photoelectron Energies and the Auger Parameter, *in* "Practical Surface Analysis by Auger and X-Ray Photoelectron Spectroscopy," D. Briggs and M.P. Seah, Eds., John Wiley & Sons, London(1983) p. 477.
66. T.P. Debies and J.W. Rabalais, *Chem. Phys.*, 20, 277(1977).
67. W.E. Morgan, W.J. Stec., and J.R. Van Wazer, *Inorg. Chem.*, 12, 953(1973).
68. G.E. McGuire, G.K. Schweitzer, and T.A. Carlson, *Inorg. Chem.*, 12, 2451(1973).
69. H.V. Doveren and J.A.T. Verhoeven, *J. Electron Spectrosc. Relat. Phenom.*, 21, 265(1980).
70. D.D. Sarma and C.N.R. Rao, *J. Electron Spectrosc. Related Phenom.*, 20, 25(1980).
71. A.F. Orchard and G. Thornton, *J. Electron Spectrosc. Relat. Phenom.*, 10, 1(1977).
72. A.F. Orchard and G. Thornton, *J. Electron Spectrosc. Relat. Phenom.*, 13, 27(1978).
73. W.-D. Schneider, C. Laubschat, I. Nowik, and G. Kaindl, *Phys. Rev. B.*, 24, 5422(1981).
74. P. Burroughs, A. Hamnett, A.F. Orchard, and G. Thornton, *J. Chem. Soc., Dalton Trans.*, 17, 1686(1976).
75. W.Y. Howng and R.J. Thorn, *Chem. Phys. Lett.*, 56, 463(1978).
76. C.K. Jorgensen and H. Berthou, *Chem. Phys. Lett.*, 13, 186(1972).
77. G.C. Bond, "Heterogeneous Catalysis," Clarendon Press, Oxford(1987).
78. C.D. Wagner, H.A. Six, W.T. Jansen, and J.A. Taylor, *Appl. Surf. Sci.*, 9, 203(1981).
79. J.A. Taylor, *J. Vac. Sci. Technol.*, 20, 751(1982).
80. T.A. Carlson, W.B. Dress, and G.L. Nyberg, *Phys. Scr.*, 16, 211(1979).
81. R. Hoogewijs, L. Fiermans, and J. Vennik, *J. Electron Spectrosc. Relat. Phenom.*, 11, 171(1977).
82. C.D. Wagner, D.E. Passoja, H.F. Hillery, T.G. Kinisky, H.A. Six, W.T. Jansen, and J.A. Taylor, *J. Vac. Sci. Technol.*, 21, 933(1982).
83. J.E. Castle and R.H. West, *J. Electron Spectrosc. Relat. Phenom.*, 18, 355(1980).
84. J.A. Taylor, *Appl. Surf. Sci.*, 7, 168(1981).
85. R.H. West and J.E. Castle, *Surf. Interface Anal.*, 4, 68(1982).
86. M. Klasson, A. Berndtsson, J. Hedman, R. Nilsson, R. Nyholm, and C. Nordling, *J. Electron Spectrosc. Relat. Phenom.*, 3, 427(1974).
87. J. Finster and P. Lorenz, *Chem. Phys. Lett.*, 50, 223(1977).
88. J.M. Adams, S. Evans, P.I. Reid, J.M. Thomas, and M.J. Walters, *Anal. Chem.*, 49, 2001(1977).
89. P.R. Anderson and W.E. Swartz, *Inorg. Chem.*, 13, 2293(1974).
90. L.S. Dake, D.R. Baer, K.F. Ferris, and D.M. Friedrich, *J. Electron Spectrosc. Relat. Phenom.*, 51, 439(1990).
91. G. Polzonetti, A. Furlani, M.V. Russo, A.M. Camus, and N. Marsich, *J. Electron Spectrosc. Relat. Phenom.*, 52, 581(1990).
92. G. Polzonetti, V. Faruffini, A. Furlani, and M.V. Russo, *Synth. Met.*, 25, 375(1988).
93. S.L. Hsu, A.J. Signorelli, G.P. Pez, and R.H. Baughman, *J. Chem. Phys.*, 69, 106(1978).

94. W.R. Salaneck, H.R. Thomas, R.W. Bigelow, C.B. Duke, E.W. Plummer, A.J. Heeger, and A.G. MacDiarmid, *J. Chem. Phys.*, 72, 3674(1980).
95. T. Hashemi and C.A. Hogarth, *Spectrochim. Acta*, 43B, 783(1988).
96. K.T. Ng and D.M. Hercules, *J. Phys. Chem.*, 80, 2095(1976).
97. M.K. Bahl, R.D. Woodall, R.L. Watson, and K.J. Irgolic, *J. Chem. Phys.*, 64, 1210(1976).
98. G. Mavel, J. Escard, P. Costa, and J. Castaing, *Surf. Sci.*, 109(1973).
99. L. Ramqvist, K. Hamrin, G. Johansson, A. Fahlmann, and C. Nordling, *J. Phys. Chem. Solids*, 30, 1835(1969).
100. G.C. Allen, M.T. Curtis, A.J. Hooper, and P.M. Tucker, *J. Chem. Soc. Dalton*, 1675(1973).
101. N.S. McIntyre and D.G. Zetaruk, *Anal. Chem.*, 49, 1521(1977).
102. W.E. Morgan and J.R. Van Wazer, *J. Phys. Chem.*, 77, 96(1973).
103. T.A. Patterson, J.C. Carver, D.E. Leyden, and D.M. Hercules, *J. Phys. Chem.*, 80, 1702(1976).
104. R.J. Colton and J.W. Rabalais, *Inorg. Chem.*, 15, 237(1976).
105. W.E. Morgan, J.R. Van Wazer, and W.J. Stec, *J. Am. Chem. Soc.*, 95, 751(1973).
106. M. Pelavin, D.N. Hendrickson, J.M. Hollander, and W.L. Jolly, *J. Phys. Chem.*, 74, 1116(1970).
107. H. Binder, *Z. für Natürforsch*, B28, 256(1973).
108. M. Murata, K. Wakino, and S. Ikeda, *J. Electron Spectrosc. Relat. Phenom.*, 6, 459(1975).
109. P. Biloen and G.T. Pott, *J. Catal.*, 30, 169(1973).
110. Y. Mizokawa, H. Iwasaki, R. Nishitani, and S. Nakamura, *J. Electron Spectrosc. Relat. Phenom.*, 14, 129(1978).
111. J. Hedman and N. Martensson, *Phys. Scr.*, 22, 176(1980).
112. R.B. Shalvoy, G.B. Fisher, and P.J. Stiles, *Phys. Rev. B*, 1680(1977).
113. C.D. Wagner, *Faraday Disc. Chem. Soc.*, 60, 291(1975).
114. L. Pederson, *J. Electron Spectrosc. Relat. Phenom.*, 28, 203(1982).
115. M.K. Bahl, R.L. Watson, and K.J. Irgolic, *J. Chem. Phys.*, 72, 4069(1980).

LAWRENCE BERKELEY LABORATORY
UNIVERSITY OF CALIFORNIA
TECHNICAL INFORMATION DEPARTMENT
BERKELEY, CALIFORNIA 94720